Time-dependent Green's function approach to spin transport assisted by nonclassical light

M. X. Bi,[1] X. H. Yan,[2,*] Y. Xiao,[1,†] and Hong Guo[3]

[1]*College of Science, Nanjing University of Aeronautics and Astronautics, Nanjing 210016, China*

[2]*School of Material Science and Engineering, Jiangsu University, Zhenjiang 212013, China*

[3]*Center for the Physics of Materials and Department of Physics, McGill University, Montreal, Quebec, Canada H3A 2T8*

(Received 27 March 2019; revised manuscript received 20 October 2019; published 17 December 2019)

The generation of spin current is of significant importance for advanced spintronic applications. In conventional theory and experiment, microwave sources are usually described by a classical time-varying field in which all fluctuations are neglected. Here, we study the spin current driven by nonclassical light by developing a Green's function method in which both effects of nonclassical light and electron-related interaction can be taken into account. Our theoretical method has more advantages than the linear response theory developed recently as it can be easily extended to the electronic transport problem with interaction. As an example, we calculate the spin current due to the rotating magnetic field in the presence of nonclassical light. It is found that the spin current is sensitive to the state of nonclassical light. Under certain conditions, the transmission and spin current can be smaller than the classical limit, which cannot be broken by a pure classical microwave field. The method developed here and the results reported here will be important for understanding complicated physical phenomena occurring in the hybrid field of spintronics and circuit quantum electrodynamics.

DOI: 10.1103/PhysRevB.100.235432

I. INTRODUCTION

Time-dependent electronic transport has attracted much interest in both theoretical and experimental physics in recent decades [1–12]. Some interesting characteristics, such as *n*-photon-assisted tunneling, have been observed experimentally or predicted theoretically [8–13]. In a number of experiments, conventional ac microwave sources are, in general, used [14–16]. To some extent, the microwave source is equivalent to a time-varying potential exerted in the device. In light of this, the microwave signal is treated as a $\cos\omega t$ function of electric potential in many theoretical calculations [1,9]. This can be regarded as a classical treatment of microwave field in which all fluctuation effects are removed.

With rapid progress in the field of quantum optics, it is now possible to prepare a photon state other than a classical state, such as the Fock state or squeezed state [17,18]. In such a case, the conventional treatment of the microwave field and the physical picture of photon-assisted tunneling should be amended. Recently, Souquet *et al.* studied theoretically electronic tunneling in a nanojunction which is illuminated with nonclassical microwave photons [8]. Some unique characteristics, which cannot be observed in pure classical microwave experiments, are predicted. As is known, the detection of nonclassical light is usually performed in the optical means. Souquet *et al.*'s work provides an alternative, i.e., an electrical means, for the detection of nonclassical light in the future.

Despite the importance of Souquet *et al.*'s work, it still can be improved in some aspects. First, electronic transport in Ref. [8] is treated within the framework of Ohm's law, i.e., $I = V/R_T$, with R_T being the resistance of the junction. Therefore, it is a semiclassical theory and is hard to use to study a pure quantum problem, such as the interference between different channels in quantum transport. To study a quantum coherent conductor, a fully quantum-mechanical method is desired. Second, it is noticed that the device in Ref. [8] consists of only the left lead and right lead. The direct coupling between two leads reproduces the tunneling current. However, as various types of interactions are present in the device, e.g., electron-electron or electron-phonon interaction, the method and device geometry in Ref. [8] make the treatment of interaction difficult. So it is important to develop a pure quantum-mechanical theory of electronic transport which can deal with both nonclassical light and the interaction effect.

Moreover, the spin-polarized transport becomes more and more important due to potential applications in the spintronic field [19–30]. Some new physical phenomena, e.g., spin pumping and spin transfer torque, and new devices, e.g., magnetic random access memory, have been proposed [31–38]. Since spin is not considered in Ref. [8], the new method developed should be able to handle the spin-related properties. Furthermore, some recent studies of spin transport are focused on the cavity-related problems in which distinct couplings, e.g., electron-spin-photon coupling [39] and magnon-photon coupling [40], are present. When cavity photons are prepared in the nonclassical states, the spin-photon coupling and nonclassical nature of photons will reproduce fascinating behavior. The study of such a problem requires the development of new theoretical tools. Based on the above, we notice that the Green's function method is a suitable one for our purpose. It has been widely used in the calculation of electronic transport problems of a quantum coherent conductor. Especially, different types of electron interactions, including spin-related

*xhyan@nuaa.edu.cn

†fryxiao@nuaa.edu.cn

interaction, can be treated by introducing the self-energy of the interaction in the Green's function method. Therefore, it is physically meaningful to develop a Green's function method for the calculation of spin transport in the presence of nonclassical light.

In this work, we develop a time-dependent Green's function method to deal with the spin current driven by the nonclassical microwave photons. Formulas of the charge and spin current are obtained which may be used to explain experimental results in the future. Moreover, the process of building the self-energy and Green's function of the Zeeman coupling between a rotating magnetic field and spin can be extended to the other interaction problems in the presence of nonclassical light, e.g., the coupling between electrons and phonons, photons, and magnons and the strong coupling between magnons and cavity photons. The results of the charge current indicate that the unique distributions of nonclassical light have an important effect on electronic transport. For example, the transmission in the case of nonclassical light can be lower than a classical limit which cannot be broken in the classical photon state. As for the spin current, the combination of spin-dependent tunneling and the nonclassical effect reproduces many phenomena which cannot be obtained in the classical case.

This paper is organized as follows. In Sec. II, we present a comprehensive derivation of the current formula for four types of photon states based on the Green's function method. After the problem without interaction is treated, we take the Zeeman interaction between spin and a time-varying magnetic field into account to show how the interaction effect is implemented in the Green's function. In Sec. III, we discuss the numerical results based on the current and transmission formulas derived in Sec. II. We focus on the effect of nonclassical light on spin transport. The findings are concluded in Sec. IV. Moreover, some cumbersome derivations are put into the Appendices.

II. THEORY AND METHOD

In this section, we describe the procedure of deriving the current formulas for various states of nonclassical light. To this end, we first present the Hamiltonian which describes the device model. An important treatment, which is different from the pure classical calculation, is the phase factor in which the photon's operator is introduced in order to describe the fluctuation. Then, the correlator arising from the phase factor is built and calculated for each state. Finally, the formulas of current and transmission are presented.

A. The Hamiltonian and Green's function

Our theoretical Hamiltonian mimics a two-probe device driven by nonclassical light that generates a time-dependent current in the microwave frequency range. It is written as

$$\hat{H} = \hat{H}_{\text{Lead}} + \hat{H}_C + \hat{H}_T, \tag{1}$$

$$\hat{H}_{\text{Lead}} = \sum_{q,\alpha=L,R} \varepsilon_{q\alpha}(t)\hat{c}^{\dagger}_{q\alpha}\hat{c}_{q\alpha}, \tag{2}$$

$$\hat{H}_C = \sum_m \varepsilon_m \hat{d}^{\dagger}_m \hat{d}_m, \tag{3}$$

$$\hat{H}_T = \sum_{q\alpha,n} V_{q\alpha,n}\hat{c}^{\dagger}_{q\alpha}\hat{d}_n + V^{*}_{n,q\alpha}\hat{d}^{\dagger}_n\hat{c}_{q\alpha}, \tag{4}$$

where $\hat{H}_{\text{Lead}}$ is the Hamiltonian of the leads of the two-probe device, $\hat{H}_C$ is the Hamiltonian of the device itself, and $\hat{H}_T$ is the coupling Hamiltonian between the leads and the device. The creation (annihilation) operator in the lead labeled by $\alpha = L, R$ is $\hat{c}^{\dagger}_{q\alpha}$ ($\hat{c}_{q\alpha}$), with q being the wave vector, and in the device it is $\hat{d}^{\dagger}_m$ ($\hat{d}_m$). In Eq. (3), ε_m is the single-particle energy of the device with quantum number m. For convenience, we consider only one energy level in the device, i.e., $\varepsilon_m = \varepsilon_0$. As shown in Eq. (4), the coupling strength between the device and the lead is given by the parameter $V_{q\alpha,n}$. The form of Eq. (4) arises from the charge conservation in the process of electronic tunneling between the lead and central region.

The time-dependent and nonclassical nature of electronic transport is represented by the single-particle energy of the leads. In general, the single-particle energy in the classical case is of the form

$$\varepsilon_{q\alpha}(t) = \varepsilon_{q\alpha 0} + eV(t), \tag{5}$$

where $V(t)$ is the oscillating voltage arising from the surrounding environment, such as the external circuit in the microwave cavity [8]. e is the elementary charge. In the treatment of the pure classical state of a microwave, it is customary to consider $V(t)$ to be the pure ac voltage, i.e., $V(t) = V_0\cos(\omega t)$. However, in nonclassical microwave states, the quantum fluctuation should be carefully considered. As studied by some other authors [8,41–47], such a quantum fluctuation will lead to fluctuation of the charge distribution in the leads and fluctuation of charge transfer across the quantum electronic conductor. In our work, the nonclassical light is introduced through these quantum fluctuations.

To describe the nonclassical light, we consider the electron's operator in the Heisenberg picture,

$$\hat{c}_{q\alpha}(t) = \hat{c}_{q\alpha 0}(t)\exp\left(-i\int_{-\infty}^{t} e\hat{V}(t_1)dt_1\right), \tag{6}$$

where the phase operator is defined as [8]

$$\hat{\varphi}(t) = e\int_{-\infty}^{t}\hat{V}(t_1)dt_1 = -i\sqrt{\rho}[\hat{a}(t) - \hat{a}^{\dagger}(t)]. \tag{7}$$

Due to quantum fluctuation, the voltage is treated as an operator $\hat{V}$ with the commutation relation $[\hat{V}(t), \hat{V}(t')] = 0$. $\hat{a}^{\dagger}$ ($\hat{a}$) is the creation (annihilation) operator of the cavity photon mode, and ρ describes the strength of the zero-point fluctuation of the cavity. Since a single level is used in the central region shown in Eq. (3), the single-mode states of the external circuit are considered in our calculations.

The Green's function of the lead is modified due to the phase factor and is rewritten as

$$g(t,t') = -i\langle T_c\hat{c}_{q\alpha}(t)\hat{c}^{\dagger}_{q\alpha}(t')\rangle = ig_{q\alpha 0}(t,t')g_{ec}(t,t'), \tag{8}$$

where we define the Green's function of the bare lead $g_{q\alpha 0}(t,t') = -i\langle T_c\hat{c}_{q\alpha 0}(t)\hat{c}^{\dagger}_{q\alpha 0}(t')\rangle$ and the Green's function of the external circuit $g_{ec}(t,t') = -i\langle T_c e^{-i\hat{\varphi}(t)}e^{i\hat{\varphi}(t')}\rangle$, respectively. Here, T_c is the time-ordering operator.

Furthermore, we define the lesser Green's function

$$g^{<}(t,t') = ig^{<}_{q\alpha 0}(t,t')g^{<}_{ec}(t,t'), \tag{9}$$

with $g^<_{ec}(t,t') = -i\langle e^{i\hat{\varphi}(t')}e^{-i\hat{\varphi}(t)}\rangle$, and the advanced Green's function

$$g^a(t,t') = g^a_{q\alpha 0}(t,t')\langle e^{i\hat{\varphi}(t')}e^{-i\hat{\varphi}(t)}\rangle + \left[g^a_2 + g^a_3\right], \tag{10}$$

with $g^a_2 = -ig^a_{q\alpha 0}(t,t')g^a_{ec}(t,t')$ and $g^a_3 = ig^<_{q\alpha 0}(t,t')g^a_{ec}(t,t')$. It can be proved that the term g^a_2 does not contribute to the current, and thus, it is omitted from now on. However, the term g^a_3 makes a contribution to the current. Further analysis shows that the current arising from this term decreases as the temperature increases. So we consider the regime where the temperature is not so low that the contribution from this term can be neglected (for details see Appendix B).

The Green's function of the bare lead, i.e., in the absence of device and electromagnetic field, takes the familiar form of [1]

$$g^<_{q\alpha 0}(t,t') = if(\varepsilon_{q\alpha 0})e^{-i\varepsilon_{q\alpha 0}(t-t')}, \tag{11}$$

$$g^a_{q\alpha 0}(t,t') = i\theta(t'-t)e^{-i\varepsilon_{q\alpha 0}(t-t')}, \tag{12}$$

where $\theta(t'-t)$ is the Heaviside step function and $f(\varepsilon_{q\alpha 0})$ is the Fermi-Dirac distribution.

B. Cavity fluctuation

In the presence of pure classical photons, the phase factor is represented by a complex number. But for nonclassical light, we have to deal with the phase factor and the correlator $\langle e^{i\hat{\varphi}(t')}e^{-i\hat{\varphi}(t)}\rangle$ quantum mechanically. For each nonclassical light with density matrix $\hat{\rho}_{cav}$, the correlator is written as

$$\langle e^{i\hat{\varphi}(t')}e^{-i\hat{\varphi}(t)}\rangle = Tr(\hat{\rho}_{cav}e^{i\hat{\varphi}(t')}e^{-i\hat{\varphi}(t)}). \tag{13}$$

We next derive the form of the correlator for each photon state.

(1) When the microwave photon is in a Fock state, i.e., $\hat{\rho}_{cav} = |n\rangle\langle n|$, the fluctuation is

$$\langle e^{i\hat{\varphi}(t')}e^{-i\hat{\varphi}(t)}\rangle = P_0(t,t')P^{\text{Fock}}_{\text{occ}}(t,t'), \tag{14}$$

where $P_0(t,t') = \sum_{k=0}^{\infty}\frac{e^{-\rho}\rho^k}{k!}e^{ik\omega(t-t')}$ is the vacuum fluctuation and ω is the frequency of the photon. $P^{\text{Fock}}_{\text{occ}}(t,t')$, which is the fluctuation arising from photon absorption (emission) when the cavity is not in the ground state [8], reads

$$P^{\text{Fock}}_{\text{occ}}(t,t') = \sum_{l=0}^{n}\frac{C^l_n}{l!}[\rho(e^{i\omega(t-t')} + e^{-i\omega(t-t')} - 2)]^l. \tag{15}$$

In the photon's ground state, $P^{\text{Fock}}_{\text{occ}}(t,t') = 1$, and thus, the vacuum fluctuation dominates the quantum fluctuation. Here, C^l_n is the binomial distribution, and $l!$ is the factorial.

(2) In the coherent state with $\hat{\rho}_{cav} = |\alpha\rangle\langle\alpha|$, the vacuum fluctuation remains unchanged, but the fluctuation $P_{\text{occ}}(t,t')$ is expressed by

$$P^{\text{coh}}_{\text{occ}}(t,t') = \sum_n\sum_m J_n(x)J_m(x)e^{in\omega t}e^{-im\omega t'}, \tag{16}$$

with $x = 2\sqrt{\rho}|\alpha|$ and J_n being the Bessel function of order n.

(3) In the thermal state, the density matrix is $\hat{\rho}_{cav} = \sum_n P_n|n\rangle\langle n|$, where $P_n = \frac{(\overline{n})^n}{(\overline{n}+1)^{n+1}}$, with $\overline{n} = \frac{1}{e^{\frac{\hbar\omega}{k_BT}}-1}$. The fluctuation is thus written as

$$P^{th}_{\text{occ}}(t,t') = e^{2\rho\overline{n}[\cos\omega(t-t')-1]}. \tag{17}$$

C. Current formula

Without the loss of generality, the time-dependent current flowing across the left lead is written as [1]

$$J_L(t) = -e\left\langle\frac{d\left(\sum_{qL}\hat{c}^\dagger_{qL}(t)\hat{c}_{qL}(t)\right)}{dt}\right\rangle = \frac{2e}{\hbar}\text{Re}\sum_{qLn}V_{qLn}G^<_{nqL}(t,t), \tag{18}$$

where Re (Im) is the real (imaginary) part of the quantity and $\hbar$ is the reduced Planck constant.

With the Green's function of the central region of the device, the current formula is given by

$$J_L(t) = J^{(1)}_L(t) + J^{(2)}_L(t), \tag{19}$$

$$\begin{aligned}J^{(1)}_L(t) = -\frac{e\Gamma^L}{\hbar}\text{Im}\Big\{i\sum_\alpha\Gamma^\alpha\int\frac{d\varepsilon}{2\pi}f_\alpha(\varepsilon)\\ \times\iint dt_1dt_2\theta(t-t_1)\theta(t-t_2)e^{-i\varepsilon(t_1-t_2)}e^{-\Gamma t}\\ \times e^{i(\varepsilon_0-\frac{i}{2}\Gamma)t_1}e^{-i(\varepsilon_0+\frac{i}{2}\Gamma)t_2}\langle e^{i\varphi(t_2)}e^{-i\varphi(t_1)}\rangle\Big\},\end{aligned} \tag{20}$$

$$\begin{aligned}J^{(2)}_L(t) = -\frac{2e\Gamma^L}{\hbar}\text{Im}\int\frac{d\varepsilon}{2\pi}f_L(\varepsilon)\int_{-\infty}^{t}dt_1\big\{-i\theta(t-t_1)\\ \times e^{i(\varepsilon_0-\frac{i}{2}\Gamma)(t_1-t)}e^{-i\varepsilon(t_1-t)}\langle e^{i\varphi(t)}e^{-i\varphi(t_1)}\rangle\big\},\end{aligned} \tag{21}$$

where $\Gamma = \Gamma^L + \Gamma^R$. Γ^L and Γ^R are the level-width functions of the left and right leads. f_L is the Fermi-Dirac distribution of the left lead. The detailed derivation of the current formula can be found in Appendix A. Next, we will discuss the current formulas for each state of nonclassical light.

1. Pure classical photon

We first consider the pure classical photon, which has been well studied [1]. Due to the absence of fluctuation, we can write $V(t) = V_0\cos(\omega t)$. Then the fluctuation becomes

$$\langle e^{i\hat{\varphi}(t_2)}e^{-i\hat{\varphi}(t_1)}\rangle_c = \sum_{m_1}\sum_{m_2}J_{m_1}(V_0/\omega)J_{m_2}(V_0/\omega)e^{im_1\omega t_1}e^{-im_2\omega t_2}. \tag{22}$$

Inserting Eq. (22) into Eq. (19) and averaging over t, the average current is

$$\left\langle J^c_L(t)\right\rangle = -\frac{e}{\hbar}\sum_{n=-\infty}^{+\infty}p^c_{\text{tot}}[n]\int\frac{d\varepsilon}{2\pi}\Gamma^R\Gamma^L\frac{f_R(\varepsilon)-f_L(\varepsilon)}{(\varepsilon-\varepsilon_0-n\omega)^2+\frac{\Gamma^2}{4}}, \tag{23}$$

where $p^c_{\text{tot}}[n] = J^2_n(V_0/\omega)$ describes the weight of total photon absorption or emission. Equation (23) is the same as those obtained in [1,9].

2. Thermal state

In the thermal state, the total fluctuation is written as

$$\begin{aligned}\langle e^{i\hat{\varphi}(t_2)}e^{-i\hat{\varphi}(t_1)}\rangle_{th} = \sum_{k_1,k_2,k_3}^{\infty}\frac{e^{-\rho}e^{-2\rho\overline{n}}\rho^{k_1}(\rho\overline{n})^{k_2+k_3}}{k_1!k_2!k_3!}\\ \times e^{i(k_1+k_2-k_3)\omega t_1}e^{-i(k_1+k_2-k_3)\omega t_2}.\end{aligned} \tag{24}$$

The average current is

$$\langle J_L^{th}(t)\rangle = -\frac{e}{\hbar}\sum_{n=k_1-k_3}^{+\infty} p_{\rm tot}^{th}[n]\int\frac{d\varepsilon}{2\pi}\Gamma^R\Gamma^L\frac{f_R(\varepsilon)-f_L(\varepsilon)}{(\varepsilon-\varepsilon_0-n\omega)^2+\frac{\Gamma^2}{4}}, \tag{25}$$

where

$$\begin{aligned} p_{\rm tot}^{th}[n] &= \sum_{k_1=0}^{+\infty} p_0[k_1]p_{\rm occ}^{th}[n-k_1] \\ &= \sum_{k_1=0}^{+\infty}\frac{e^{-\rho}\rho^{k_1}}{k_1!}\sum_{k_3=0}^{+\infty}\frac{e^{-2\rho\bar{n}}(\rho\bar{n})^{n-k_1+2k_3}}{(n-k_1+k_3)!k_3!}, \end{aligned} \tag{26}$$

in which $p_{\rm tot}^{th}[n]$ represents the weight of total photon absorption or emission, $p_0[k_1]$ describes the probability of k_1-photon absorption by the cavity in the ground state, and $p_{\rm occ}^{th}[n-k_1]$ is a quasiprobability of an additional $(n-k_1)$-photon absorption or emission process when the cavity is not in the ground state.

3. Coherent state

In the coherent state, the fluctuation is determined by both vacuum fluctuation and photon occupation fluctuation and reads

$$\begin{aligned} &\langle e^{i\hat{\varphi}(t_2)}e^{-i\hat{\varphi}(t_1)}\rangle_{\rm coh} \\ &= \sum_{k=0}^{\infty}\frac{e^{-\rho}\rho^k}{k!}\sum_n\sum_m J_nJ_m e^{i(n+k)\omega t_1}e^{-i(m+k)\omega t_2}. \end{aligned} \tag{27}$$

The average current is

$$\begin{aligned} \langle J_L^{\rm coh}(t)\rangle &= -\frac{e}{\hbar}\sum_{n=-\infty}^{+\infty} p_{\rm tot}^{\rm coh}[n] \\ &\times\int\frac{d\varepsilon}{2\pi}\Gamma^R\Gamma^L\frac{f_R(\varepsilon)-f_L(\varepsilon)}{(\varepsilon-\varepsilon_0-n\omega)^2+\frac{\Gamma^2}{4}}, \end{aligned} \tag{28}$$

where

$$p_{\rm tot}^{\rm coh}[n] = \sum_{k=0}^{+\infty} p_0[k]p_{\rm occ}^{\rm coh}[n-k] = \sum_{k=0}^{+\infty}\frac{e^{-\rho}\rho^k}{k!}J_{n-k}^2. \tag{29}$$

4. Fock state

In the Fock state, the fluctuation is written as

$$\langle e^{i\hat{\varphi}(t_2)}e^{-i\hat{\varphi}(t_1)}\rangle_{Fock} = \sum_{n\geqslant -k}^{+\infty} p_{{\rm tot},k}^{\rm Fock}[n]e^{-in\omega(t_2-t_1)}, \tag{30}$$

where

$$p_{{\rm tot},k}^{\rm Fock}[n] = \frac{e^{-\rho}\rho^n k!}{(k+n)!}\left[L_k^{(n)}(\rho)\right]^2, \tag{31}$$

in which $L_k^{(n)}(\rho)$ is the generalized Laguerre polynomial.

The average current is thus given by

$$\begin{aligned} \langle J_L^{\rm Fock}(t)\rangle &= -\frac{e}{\hbar}\sum_{n\geqslant -k}^{+\infty} p_{{\rm tot},k}^{\rm Fock}[n] \\ &\times\int\frac{d\varepsilon}{2\pi}\Gamma^R\Gamma^L\frac{f_R(\varepsilon)-f_L(\varepsilon)}{(\varepsilon-\varepsilon_0-n\omega)^2+\frac{\Gamma^2}{4}}. \end{aligned} \tag{32}$$

D. Spin current

As mentioned in Introduction, the merit of the Green's function method is the ability of treating the interaction in electronic transport calculation. Here, we consider the Zeeman coupling between a rotating magnetic field and the spin to see how both interaction and nonclassical effects are treated in the Green's function method. The rotating magnetic field takes the form of $\vec{B} = B_0(\sin\theta\cos\omega t\,\vec{i} + \sin\theta\sin\omega t\,\vec{j} + \cos\theta\,\vec{k})$, where θ is the angle between rotating magnetic field and the z axis. The Hamiltonian consists of the terms in the absence of Zeeman interaction, i.e., Eq. (1), and the terms with Zeeman interaction written as

$$H_{\rm zeeman} = \gamma_c[\hat{d}_\uparrow^\dagger\hat{d}_\uparrow - \hat{d}_\downarrow^\dagger\hat{d}_\downarrow] + \gamma_s[e^{-i\omega t}\hat{d}_\uparrow^\dagger\hat{d}_\downarrow + e^{i\omega t}\hat{d}_\downarrow^\dagger\hat{d}_\uparrow], \tag{33}$$

where $\gamma_c = B_0\cos\theta$ and $\gamma_s = B_0\sin\theta$.

The current operator of the α lead in spin space is written as [19]

$$\hat{I}_{\alpha\sigma\sigma'} = -i\sum_q[V_{k\alpha}\hat{c}_{q\alpha\sigma}^\dagger\hat{d}_{\sigma'} - V_{q\alpha}^*\hat{d}_\sigma^\dagger\hat{c}_{q\alpha\sigma'}]. \tag{34}$$

In order to obtain the spin current, we consider the self-energy arising from the Zeeman interaction based on the nonequilibrium Green's function theory. Detailed derivations can be found in Appendix C. The spin current obtained is written as

$$\begin{aligned} &\langle\hat{I}_{\alpha,\uparrow\uparrow}^\nu(t)\rangle \\ &= -\langle\hat{I}_{\alpha,\downarrow\downarrow}^\nu(t)\rangle \\ &= \sum_n^\infty p_{\rm tot}^\nu[n]\Gamma\Gamma^\alpha\int\frac{dE}{2\pi}\left|\frac{\gamma_s G_{\downarrow\downarrow}^{0r}(E)G_{\uparrow\uparrow}^{0r}(E+\omega)}{1-\gamma_s^2 G_{\downarrow\downarrow}^{0r}(E)G_{\uparrow\uparrow}^{0r}(E+\omega)}\right|^2 \\ &\quad\times[f(E+n\omega)-f(E+\omega+n\omega)], \end{aligned} \tag{35}$$

where ν denotes pure classical, thermal, coherent, and Fock states. The explicit forms of $G_{\uparrow\uparrow}^{0r}$ and $G_{\downarrow\downarrow}^{0r}$ are given in Appendix C.

III. NUMERICAL RESULTS AND DISCUSSION

With the formulas of the current, Eqs. (23), (25), (28), and (32), we calculate the transmission coefficient (integrand in the current formula) numerically. We discuss the results in two cases, i.e., the nonspin polarization and spin polarization.

A. Nonspin polarization

Figure 1 shows the transmission coefficient as a function of energy for each state of the microwave. First, as shown in Fig. 1(a), one can see that for a pure classical microwave

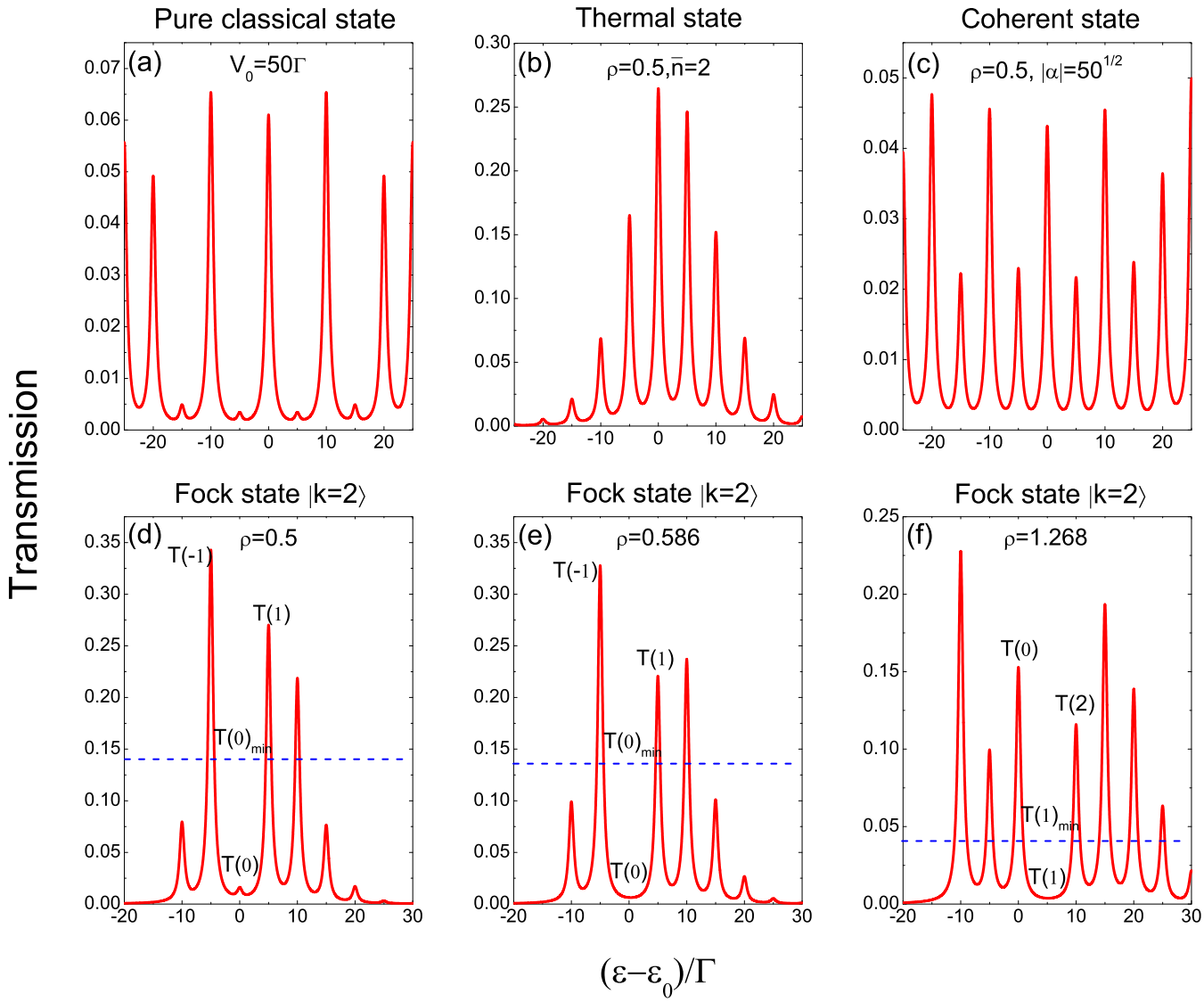

FIG. 1. Transmission coefficient versus $(\varepsilon - \varepsilon_0)/\Gamma$ with $\omega/\Gamma = 5$ for each cavity state. (a), (b), and (c) correspond to the pure classical state, coherent state, and thermal state, respectively. (d), (e), and (f) are Fock states $|k = 2\rangle$ with different ρ. The blue dashed line represents the classical limit.

the transmission presents many resonance tunneling peaks located at

$$(\varepsilon - \varepsilon_0)/\Gamma = n\omega/\Gamma, \quad n = 0, 1, 2, \ldots. \tag{36}$$

These peaks have been well studied in the literature [1,10] and are attributed to the classical photon-assisted tunneling. Each peak represents the contribution from the n-photon absorption or emission process. We also notice that the main peak ($\varepsilon = \varepsilon_0$) has a lower height than some other side peaks due to the oscillation of the Bessel function and large microwave amplitude [9]. A unique feature of the pure classical microwave state is the symmetry of transmission with respect to $\varepsilon = \varepsilon_0$. This feature is absent in all other microwave photon states. As for the thermal state, the transmission is no longer symmetric. Compared to the pure classical microwave, the heights of the main and side peaks present a Poisson distribution which can be appreciated from the distribution functions in Eq. (26). But for the coherent state, the transmission is distinct from both pure classical and thermal states. First, no Poisson distribution is shown for the main and side peaks. Second, compared to the pure classical state, the transmission is not symmetric. More important, some photon-assisted tunneling, which is very weak in the pure classical state [e.g., one- and three-photon-assisted tunneling shown in Fig. 1(a)], becomes large in the coherent state. This is a consequence of vacuum fluctuation and represents a signature which cannot be observed in the conventional pure classical microwave.

We next discuss the Fock state shown in Figs. 1(d)–1(f). As $\rho = 0.5$, a striking behavior is that the main peak becomes very small, which is not seen in the other three photon states. This indicates that the resonant process contributes little to electronic tunneling. As ρ increases further, as shown in Fig. 1(e), the contribution arising from the resonant tunneling is almost zero. This cannot be explained based on the classical tunneling theory and thus could be regarded as a nonclassical effect. In order to further demonstrate the effect of a

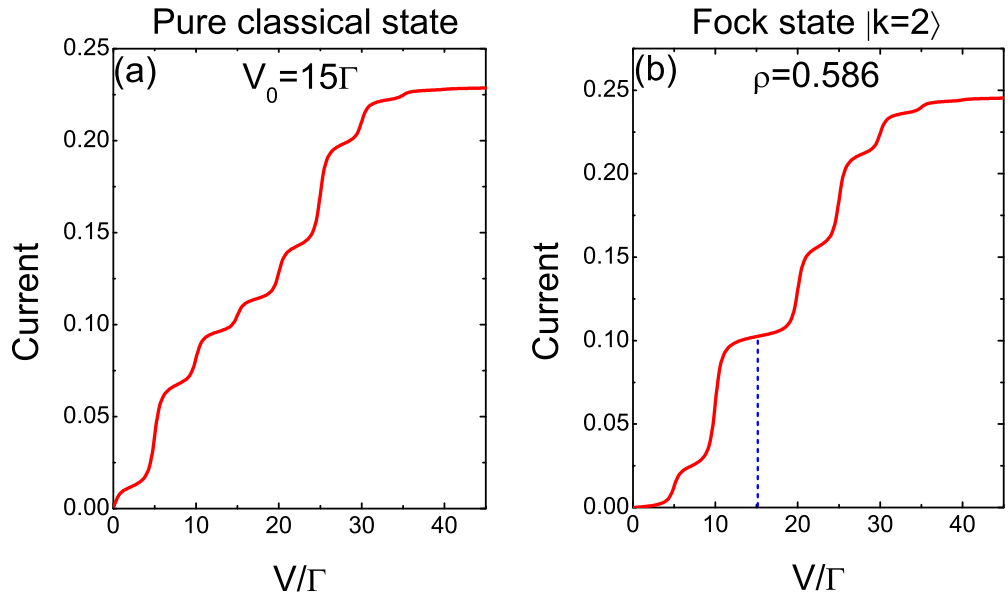

FIG. 2. Current (in units of $e\Gamma/\hbar$) as a function of V/Γ with $\omega/\Gamma = 5$. The parameters in (a) and (b) are the same as those in Figs. 1(a) and 1(e), respectively.

nonclassical microwave, we adopt the method proposed by Souquet *et al.* to calculate the classical limit, which is a lower bound of the transmission coefficient for a classical microwave. Such a limit can be broken only in the nonclassical case and is described here by an inequality (for details see Ref. [8]),

$$\begin{aligned} T(0) > {} & \frac{T(1)+T(-1)}{2} - \frac{1}{4}p_0[1] - \frac{1}{4}(p_0[1] \\ & + p_0[2])\Delta + \left\{p_0[0] - \frac{1}{4}p_0[1] + \left(\frac{5}{4}p_0[1]\right.\right. \\ & \left.\left. - p_0[0] - \frac{1}{4}p_0[2]\right)\Delta\right\}p_{\rm occ}[0] + \left\{\frac{3}{2}p_0[1]\right. \\ & - p_0[0] - \frac{1}{2}p_0[2] + \left(2p_0[0] - p_0[1] + \frac{3}{2}p_0[2]\right. \\ & \left.\left. - \frac{1}{2}p_0[3]\right)\Delta\right\}p_{\rm occ}[1] + \left(\frac{3}{2}p_0[1] - p_0[2] - \frac{1}{2}p_0[0]\right. \\ & \left. + \frac{1}{2}p_0[3] - \frac{1}{2}p_0[4]\right)\Delta p_{\rm occ}[2], \end{aligned} \tag{37}$$

where $\Delta = \frac{1}{4(\omega/\Gamma)^2+1}$. Inserting the constraint condition

$$\begin{aligned} \sum_{n=-\infty}^{+\infty} p_{\rm occ}[n] = 1, \\ p_{\rm occ}[n] = p_{\rm occ}[-n] \end{aligned} \tag{38}$$

into Eq. (37), one can obtain the minimum $T(0)_{\rm min}$. The limit is represented by the blue dashed line in Figs. 1(d)–1(f). It represents the lowest value of the transmission coefficient which can be achieved for the classical state. But $T(0)$ of the Fock state is much smaller than this limit. When looking at the current formula, i.e., Eq. (32), we can find that the above nontrivial behavior actually arises from the negativity of $p_{\rm occ}[n]$. So we can tune the value of ρ to make any n-photon-assisted tunneling vanish. For example, for $\rho = 1.268$, shown in Fig. 1(f), the first generalized Laguerre polynomial $L_k^{(n)}(\rho)$ is zero, and thus, $p_{\rm occ}[1]$ becomes negative. In such a case, $T(1)$ is below the classical limit $T(1)_{\rm min}$.

Figure 2 shows the average current versus bias voltage which is calculated from the integration of the transmission coefficient. As for the pure classical microwave, the current presents steps at bias voltage $V/\Gamma = n\omega/\Gamma$ corresponding to n-photon-assisted tunneling. When the photon is in the $|k = 2\rangle$ Fock state with $\rho = 0.586$, the step at $V/\Gamma = 15$ vanishes due to the negative quasiprobability distribution $p_{\rm occ}[k]$. The absence of some steps in the current-bias relation is directly related to the nonclassical nature of the microwave photon. Therefore, it may be used to discriminate the nonclassical feature of microwave photons in future experiments of circuit quantum electrodynamic dynamics.

Here, we will make some comments on the similarities and differences between our work and Ref. [8]. First, in our work, the Green's function method produces results physically consistent with the linear response theory of Ref. [8]. This indicates that it is feasible to employ the Green's function method in the electronic transport calculations in the presence of a nonclassical microwave. Second, the power of the Green's function method is in the problem of interaction between electron and other quasiparticles. So in the next section, we will present the numerical results of the effect of the Zeeman interaction on the spin current.

B. Spin polarization

To better understand the results of spin polarization, we divide the total transmission into two parts, i.e.,

$$T(E) = \xi(E)\chi(E), \tag{39}$$

where

$$\xi(E) = \Gamma\Gamma^{\alpha}\left|\frac{\gamma_s G^{0r}_{\uparrow\uparrow}(E+\omega)G^{0r}_{\downarrow\downarrow}(E)}{1-\gamma_s^2 G^{0r}_{\uparrow\uparrow}(E+\omega)G^{0r}_{\downarrow\downarrow}(E)}\right|^2 \tag{40}$$

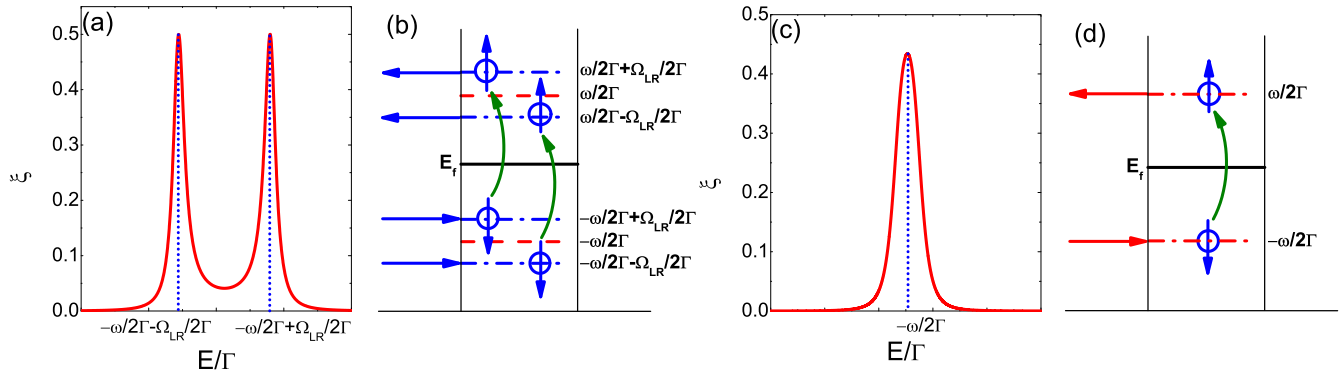

FIG. 3. (a) ξ versus energy E/Γ and (b) schematic of spin current generation in the weak-coupling regime. (c) and (d) The same as (a) and (b), but for the strong-coupling regime.

and

$$\chi(E) = \sum_{n}^{+\infty} p^{v}_{\rm tot}[n][f(E+n\omega) - f(E+\omega+n\omega)]. \quad (41)$$

In these two terms, the function ξ determines the contribution of spin-polarized electron tunneling, while the function $\chi(E)$ is the contribution of nonclassical microwave photons. We first discuss the characteristics of the function ξ.

For convenience, the ξ function is further simplified with the expressions of G^{0r} and can be written as

$$\xi = \frac{\Gamma\Gamma^{\alpha}\gamma_s^2}{\left[(E-\varepsilon_0)^2 + \omega(E-\varepsilon_0) + \frac{\omega^2-\Omega_{LR}^2}{4}\right]^2 + \frac{\Gamma^2}{4}\Omega_{LR}^2 + \frac{\Gamma^4}{4}}. \quad (42)$$

The discussion can focus on two regimes according to the quantity $\Omega_{LR}^2 = (2B_0\cos\theta - \omega)^2 + 4\gamma_s^2 - \Gamma^2$. The first one is the weak-coupling regime with $\Omega_{LR}^2 > 0$, i.e., the coupling between the device and the lead is relatively weak. From Eq. (42), one can see that the function ξ reaches the maximum at

$$E = \varepsilon_0 - \frac{\omega}{2} \pm \frac{\Omega_{LR}}{2}. \quad (43)$$

In the terminology of quantum optics, Ω_{LR} can be regarded as the Rabi frequency, indicating the oscillation of electrons between spin-up and spin-down dressed energy levels [20]. The Rabi oscillation splits the original spin-down level, causing $E = \varepsilon_0 - \frac{\omega}{2}$ to be $E = \varepsilon_0 - \frac{\omega}{2} \pm \frac{\Omega_{LR}}{2}$. The same holds for the spin-up level; that is, $E = \varepsilon_0 + \frac{\omega}{2}$ changes to $E = \varepsilon_0 + \frac{\omega}{2} \pm \frac{\Omega_{LR}}{2}$. The numerical results of the function ξ are plotted in Fig. 3(a). The two peaks are well described by the above analytic expressions. Figure 3(b) depicts the schematic diagram of a two-channel spin-dependent tunneling process. One spin-down electron with incident energy $E = -\frac{\omega}{2} + \frac{\Omega_{LR}}{2}$ tunnels into the device from the left lead; it absorbs a photon with frequency ω and then transits to the spin-up dressed energy level ($E = \frac{\omega}{2} + \frac{\Omega_{LR}}{2}$) with a spin flip. Finally, this spin-up electron tunnels out of the device to the left lead. Another spin-down electron has a similar tunneling process, but with incident energy $E = -\frac{\omega}{2} - \frac{\Omega_{LR}}{2}$. Therefore, a spin current is produced in the left lead, but the charge current remains zero over the whole process.

The second regime is the strong-coupling regime which occurs when $\Omega_{LR}^2 < 0$; that is, the coupling between the device and lead is strong. In such a case, there is no solution for the condition of $\Omega_{LR}^2 < 0$. So there is only one maximum for the function ξ, which takes place at

$$E = \varepsilon_0 - \frac{\omega}{2}. \quad (44)$$

Figure 3(c) shows the function ξ versus the energy in the strong-coupling regime. As expected, there is only one peak and thus only one spin tunneling channel. In this regime, the tunneling process shown in Fig. 3(d) indicates that a spin-down electron with energy $E = -\frac{\omega}{2}$ enters the device from the left lead and leaves the device and goes back to the left or right lead with a spin flip.

The second part is the function χ, which reflects the contribution of the nonclassical microwave. The results of the function χ are shown in Fig. 4. For the sake of comparison, the function ξ is also given by the red line. Figures 4(a)–4(d) are for the strong-coupling regime in which no Rabi splitting is present. So one can see only one peak in the function ξ. Like for the pure classical state, the function χ displays an oscillating behavior which arises from the oscillation of the Bessel function. For the thermal state, the curve of χ is similar to the Poisson distribution, as expected. But for the coherent state, the function χ is similar to the pure classical state, but the height of the step becomes smaller. This is due to the contribution of vacuum fluctuation in the coherent state. Like for the Fock state $|n=2\rangle$ with $\rho = 0.5$, the function χ presents interesting characteristics. One can see that the probability of resonant tunneling, i.e., $p_{\rm tot}[0]$, is much smaller than that of nonzero-photon-assisted events. Here, we give the classical limit in the case of spin polarization,

$$\begin{aligned} p_{\rm tot}[0] > {} & \frac{p_{\rm tot}[1] + p_{\rm tot}[-1]}{2} - \frac{1}{4}p_0[1] \\ & + \left(p_0[0] - \frac{1}{4}p_0[1]\right)p_{\rm occ}[0] \\ & + \left(\frac{3}{2}p_0[1] - p_0[0] - \frac{1}{2}p_0[2]\right)p_{\rm occ}[1]. \end{aligned} \quad (45)$$

In Fig. 4(d), $p_{\rm tot}[0]$ is below the classical limit, which indicates the effect of the nonclassical Fock state on electronic

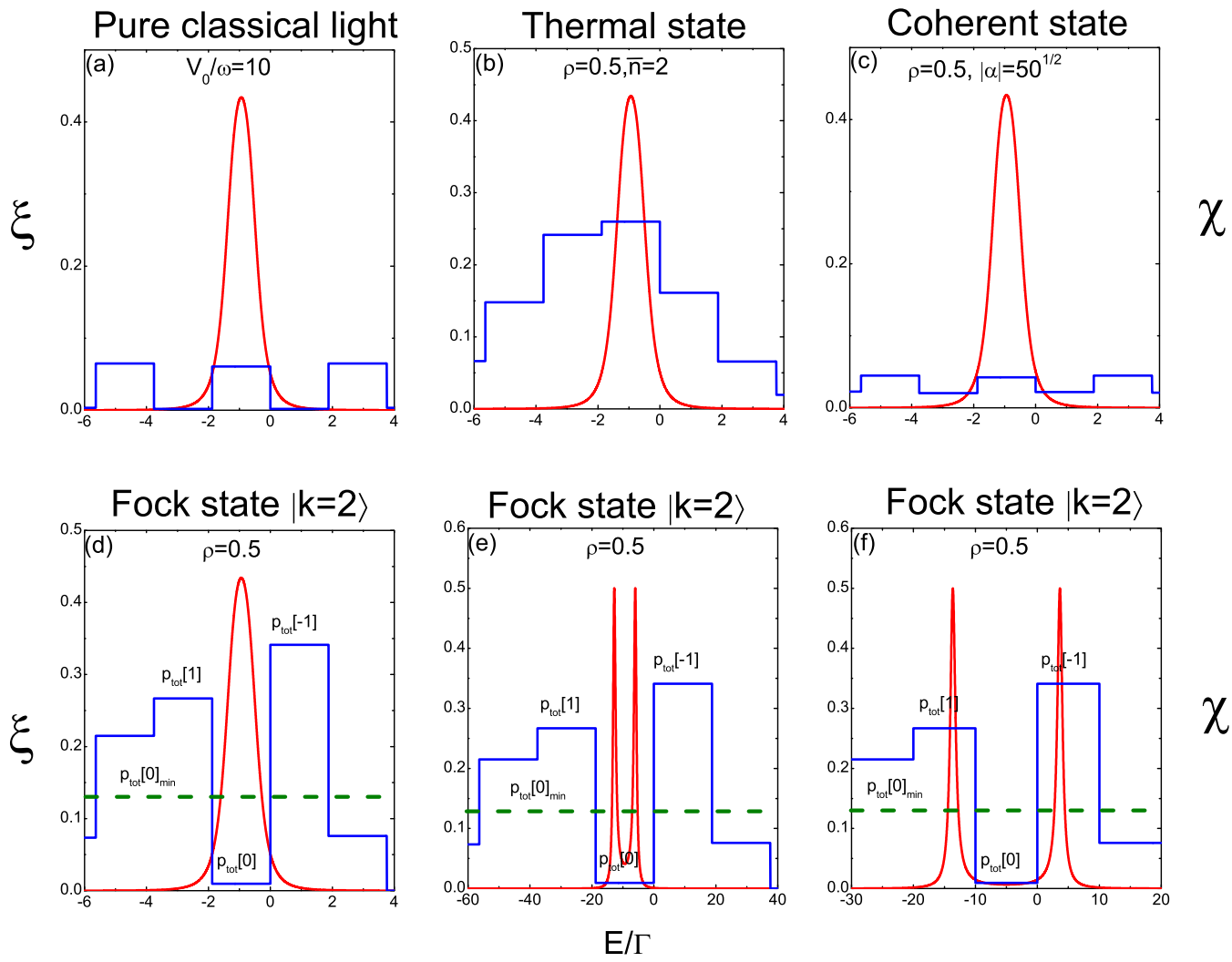

FIG. 4. ξ (red line) and χ (blue line) versus energy E/Γ for various photon states. (a)–(d) are for the strong-coupling regime with parameters $\varepsilon_0/\Gamma = 0$, $B_0/\Gamma = 1$, $\theta = 20^\circ$, and $\omega/\Gamma = 1.88$. (e) is for the weak-coupling regime with parameters $\varepsilon_0/\Gamma = 0$, $B_0/\Gamma = 10$, $\theta = 20^\circ$, and $\omega/\Gamma = 18.8$. (f) is also for the weak-coupling regime but with parameters $\varepsilon_0/\Gamma = 0$, $B_0/\Gamma = 10$, $\theta = 60^\circ$, and $\omega/\Gamma = 10$. The dashed line represents the classical limit.

tunneling. As mentioned above, such behavior arises from the negativity of $p_{\rm occ}[k]$, which is always positive in classical states.

Since the transmission coefficient is determined by both ξ and χ, we next discuss the behavior of ξ and χ at some energy interval. To this end, we label $p_{\rm tot}[n]$ in each step of Figs. 4(d)–4(f). Here, we focus on $p_{\rm tot}[n]$ with $n = 0, \pm 1$ due to the relatively large contribution. In the strong-coupling regime shown in Fig. 4(d), the function ξ is very small in the region where $p_{\rm tot}[\pm 1]$ dominates. Therefore, only the region of $p_{\rm tot}[0]$ is needed in the transmission calculation. In this region, the function ξ is large, but the function χ corresponding to $p_{\rm tot}[0]$ is negligibly small. So the transmission coefficient is small, and the spin current is suppressed in this case. In the weak-coupling regime, there are two possibilities corresponding to small and large Rabi splittings. For small Rabi splitting, as shown in Fig. 4(e), the two peaks of the function ξ are close and stay in the region of $p_{\rm tot}[0]$. Because the function χ is small, the transmission coefficient is small as well. However, for large Rabi splitting that is larger than the photon frequency, the two peaks of the function ξ are no longer within the range of $p_{\rm tot}[0]$ but stay in the region of $p_{\rm tot}[\pm 1]$. As seen in Fig. 4(f), the function χ corresponding to $p_{\rm tot}[\pm 1]$ is large. In such a case, both the nonclassical effect and spin effect contribute to the transmission coefficient significantly. Based on these results, one can see that, as the nonclassical microwave is used in experiment, one can achieve both high-spin-current and low-spin-current states by tuning either the photon frequency ω or the amplitude of the rotating magnetic field B_0.

Figure 5(a) shows the spin current as a function of photon frequency for three different photon states. As the photon frequency is low, the spin currents of the three photon states are close, and thus enlarged views are shown in Figs. 5(b) and 5(c). In the low-frequency region shown in Fig. 5(b), the spin current of the pure classical state is the largest among the three states. In order to explain this behavior, we plot the variation of ξ and χ in Fig. 5(d). When the photon frequency takes a small value of 0.2Γ, the Rabi splitting is large, and the spin current depends on the distribution of χ. Compared to

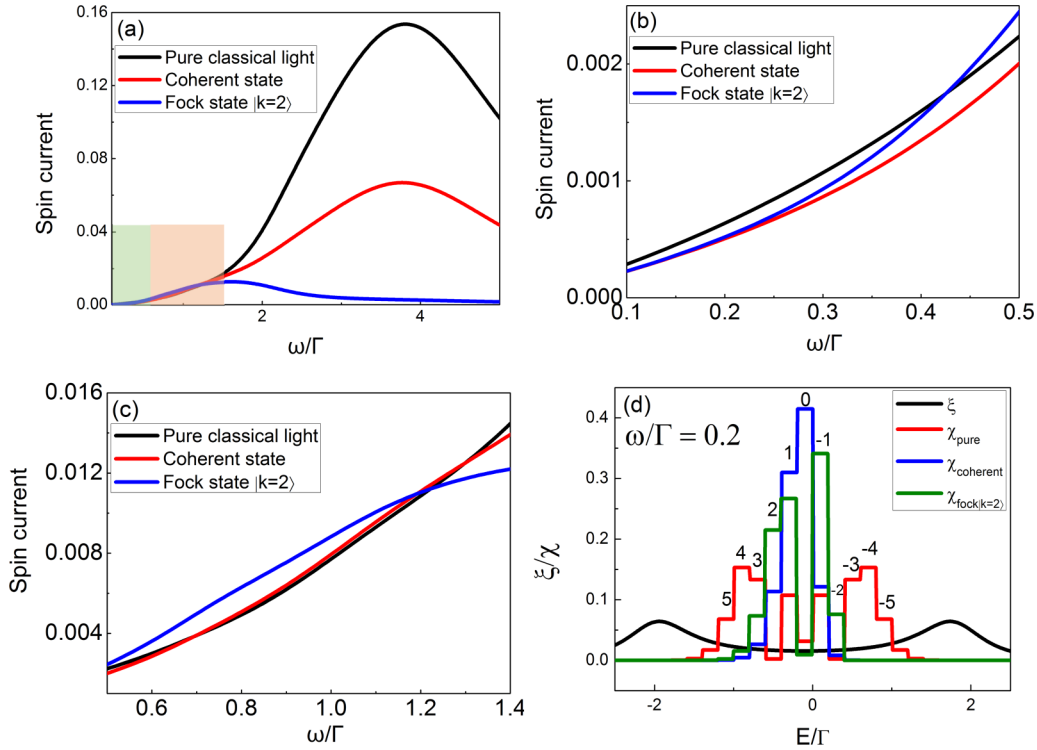

FIG. 5. (a) Spin current of three photon states as a function of photon frequency. (b) and (c) are enlarged views of (a) in the low-frequency parts defined by the shaded region. The parameters used are $\varepsilon_0/\Gamma = 0$, $B_0/\Gamma = 2$, $\theta = 20^\circ$. Moreover, $V_0 = \Gamma$ for the pure classical state; $\rho = 0.5$ and $|\alpha| = \sqrt{0.5}$ for the coherent state. (d) ξ and χ versus energy for a low photon frequency.

the Fock state and coherent state, the classical state is widely distributed and can take a larger value of ξ. On the contrary, the other two states are concentrated within the region where ξ is close to zero. As the photon frequency increases, the spin current of the Fock state increases rapidly. At some frequency, the Fock state dominates over the other two states. This could be explained based on Fig. 4(f), in which both ξ and χ are large. As photon frequency increases further, as shown in Fig. 5(c), the spin current of the Fock state decreases since the small $p_{\rm tot}[0]$ dominates the current. This has been demonstrated in Fig. 4(e). The above results reveal the roles played by the spin-dependent tunneling and the distribution of nonclassical light. We expect that future experiments can be performed to observe the above phenomena.

IV. SUMMARY

In summary, we investigated the novel physics of spin current assisted by nonclassical microwave photons by developing a time-dependent Green's function method. First, the Green's function method was extended from the case of a pure classical state, which has been well studied for several decades, to the case with a nonclassical state. With some approximations used, a current formula of nonspin-polarized tunneling was obtained in which the effect of nonclassical light manifests itself with a correlator. Most important, the method developed here was used for the problem of spin current under the excitation of a rotating magnetic field. This makes possible the application of the Green's function method in the circuit quantum electrodynamics with strong electron-photon or electron-phonon interactions. Second, the spin current presents new characteristics in the presence of nonclassical microwave photons. Our results show that the spin current is determined by both the spin electron tunneling and the state of nonclassical light. By tuning the amplitude or the direction of the magnetic field, we can arrive at the strong- or weak-coupling regime. In the strong-coupling regime, as the nonclassical microwave photons are used, the spin current depends on the Rabi splitting. That is to say, the spin current can be improved when the peak corresponding to n-photon-assisted tunneling coincides with the region with high probability of photon absorption or emission. Moreover, due to the negativity of the photon occupation distribution, the transmission and spin current can be smaller than the classical limit. This represents a genuine nonclassical-light-assisted electronic transport. The above feature can be used both to detect the nonclassical microwave for quantum manipulation applications and to tune the spin current for spintronic applications.

ACKNOWLEDGMENTS

This work is supported by the National Natural Science Foundation of China (Grants No. NSFC91750112, No. 61974067, and No. 11804158).

APPENDIX A: THE TIME-DEPENDENT CURRENT

In this Appendix, we give a detailed derivation of the time-dependent current in the presence of nonclassical microwave photons based on the Green's function method. First, based on Ref. [1], the time-dependent current flowing across the left

lead can be written as

$$J_L(t) = -e\left\langle \frac{d\left[\sum_{qL}\hat{c}^{\dagger}_{qL}(t)\hat{c}_{qL}(t)\right]}{dt}\right\rangle = \frac{2e}{\hbar}Re\sum_{qLn}V_{qLn}G^{<}_{nqL}(t,t). \tag{A1}$$

By defining the Green's function $G_{nqL}(t,t') = -i\langle T_c[\hat{d}_n(t)\hat{c}^{\dagger}_{qL}(t')]\rangle$, we get

$$G^{<}_{nqL}(t,t') = \sum_m \int dt_1 V_{mkL}\left[G^{R}_{nm}(t,t_1)g^{<}_{qL}(t_1,t') + G^{<}_{nm}(t,t_1)g^{a}_{qL}(t_1,t')\right]. \tag{A2}$$

With the help of Eqs. (9)–(12), Eq. (A2) becomes

$$G^{<}_{nqL}(t,t) = i\sum_m \int dt_1 V_{mqL}e^{-i\varepsilon(t_1-t)}\langle e^{i\hat{\varphi}(t)}e^{-i\hat{\varphi}(t_1)}\rangle \times\left[G^{R}_{nm}(t,t_1)f(\varepsilon) + \theta(t-t_1)G^{<}_{nm}(t,t_1)\right], \tag{A3}$$

where $G^{R,<}_{nm}(t,t_1)$ is the lesser Green's function of the central region. Using Eq. (A3), Eq. A(1) can be rewritten as

$$\begin{aligned} J_L(t) &= -\frac{2e}{\hbar}\mathrm{Im}\sum_{qLnm}V_{qLn}\int_{-\infty}^{t}dt_1 V_{mqL}e^{-i\varepsilon(t_1-t)} \times\langle e^{i\hat{\varphi}(t)}e^{-i\hat{\varphi}(t_1)}\rangle\left[G^{R}_{nm}(t,t_1)f(\varepsilon) + G^{<}_{nm}(t,t_1)\right] \\ &= -\frac{2e}{\hbar}\mathrm{Im}\int_{-\infty}^{t}dt_1\int\frac{d\varepsilon}{2\pi}\Gamma_L e^{-i\varepsilon(t_1-t)}\langle e^{i\hat{\varphi}(t)}e^{-i\hat{\varphi}(t_1)}\rangle \times \mathrm{Tr}[\mathbf{G}^{R}(t,t_1)f(\varepsilon) + \mathbf{G}^{<}(t,t_1)], \end{aligned} \tag{A4}$$

where $[\Gamma_L(\varepsilon)]_{mn} = 2\pi\rho(\varepsilon)V_{m,qL}V_{qL,n}$ is the level-width function of the left lead. Under the wide-band-limit approximation, we have $\mathbf{\Gamma}_L(\varepsilon) = \Gamma_L$.

In the presence of a nonclassical microwave, the forms of the Keldysh equation and Dyson equation do not change, i.e.,

$$\mathbf{G}^{<}(t,t') = \iint dt_1 dt_2 \mathbf{G}^{R}(t,t_1)\mathbf{\Sigma}^{<}(t_1,t_2)\mathbf{G}^{A}(t_2,t'), \tag{A5}$$

$$\mathbf{G}^{R}(t,t') = \mathbf{G}^{R}_0(t,t') + \iint dt_1 dt_2 \mathbf{G}^{R}_0(t,t_1)\mathbf{\Sigma}^{R}(t_1,t_2)\mathbf{G}^{R}(t_2,t'). \tag{A6}$$

However, the lesser self-energy takes a new form,

$$\Sigma^{<}(t_1,t_2) = i\sum_{\alpha}\int\frac{d\varepsilon}{2\pi}\Gamma^{\alpha}f_{\alpha}(\varepsilon)e^{-i\varepsilon(t_1-t_2)}\langle e^{i\hat{\varphi}(t_2)}e^{-i\hat{\varphi}(t_1)}\rangle, \tag{A7}$$

and the retarded self-energy is

$$\Sigma^{R}(t_1,t_2) = -i\sum_{\alpha}\int\frac{d\varepsilon}{2\pi}\Gamma^{\alpha}\theta(t_1-t_2)e^{-i\varepsilon(t_1-t_2)}\langle e^{i\hat{\varphi}(t_2)}e^{-i\hat{\varphi}(t_1)}\rangle. \tag{A8}$$

Due to $\int\frac{d\varepsilon}{2\pi}e^{i\varepsilon t} = \delta(t)$ and $\langle e^{i\hat{\varphi}(t)}e^{-i\hat{\varphi}(t)}\rangle = 1$, we have

$$\Sigma^{R}(t_1,t_2) = -\frac{i}{2}\Gamma\delta(t_1-t_2), \tag{A9}$$

where $\Gamma = \Gamma^L + \Gamma^R$.

Following Ref. [1], the solution of Eq. (A6) can be written as

$$G^{R}(t,t') = -i\theta(t-t')e^{i(\varepsilon_0-\frac{i}{2}\Gamma)(t'-t)}. \tag{A10}$$

Finally, we have the current formula

$$J_L(t) = J^{(1)}_L(t) + J^{(2)}_L(t), \tag{A11}$$

$$J^{(1)}_L(t) = -\frac{e\Gamma^L}{\hbar}\mathrm{Im}\left\{i\sum_{\alpha}\Gamma^{\alpha}\int\frac{d\varepsilon}{2\pi}f_{\alpha}(\varepsilon) \times\iint dt_1 dt_2\theta(t-t_1)\theta(t-t_2)e^{-i\varepsilon(t_1-t_2)}e^{-\Gamma t} \times e^{i(\varepsilon_0-\frac{i}{2}\Gamma)t_1}e^{-i(\varepsilon_0+\frac{i}{2}\Gamma)t_2}\langle e^{i\hat{\varphi}(t_2)}e^{-i\hat{\varphi}(t_1)}\rangle\right\}, \tag{A12}$$

$$J^{(2)}_L(t) = -\frac{2e\Gamma^L}{\hbar}\mathrm{Im}\int\frac{d\varepsilon}{2\pi}f_L(\varepsilon)\int_{-\infty}^{t}dt_1\left\{-i\theta(t-t_1) \times e^{i(\varepsilon_0-\frac{i}{2}\Gamma)(t_1-t)}e^{-i\varepsilon(t_1-t)}\langle e^{i\hat{\varphi}(t)}e^{-i\hat{\varphi}(t_1)}\rangle\right\}, \tag{A13}$$

where the effect of the cavity fluctuation has been introduced.

APPENDIX B: INFLUENCE OF g^a_2 AND g^a_3 ON THE CURRENT

In this Appendix, we will discuss the contribution from two terms, i.e., $g^a_2(t,t')$ and $g^a_3(t,t')$, which are neglected in the main text.

We first consider $g^a_2(t,t')$, which is written as

$$\begin{aligned} g^a_2(t,t') &= -ig^a_{q\alpha 0}(t,t')g^a_{ec}(t,t') \\ &= i\theta(t'-t)\theta(t'-t)e^{-i\varepsilon_{q\alpha 0}(t-t')} \\ &\quad[\langle e^{-i\hat{\varphi}(t)}e^{i\hat{\varphi}(t')}\rangle - \langle e^{i\hat{\varphi}(t')}e^{-i\hat{\varphi}(t)}\rangle]. \end{aligned} \tag{B1}$$

By virtue of Eqs. (10) and (19), we can write the current, which is contributed by $g^a_2(t,t')$ as

$$J^{g^a_2}_L(t) = -\frac{e\Gamma^L}{2\hbar}\mathrm{Im}G^{<}(t,t)[\langle e^{-i\hat{\varphi}(t)}e^{i\hat{\varphi}(t)}\rangle - \langle e^{i\varphi(t)}e^{-i\varphi(t)}\rangle]. \tag{B2}$$

Due to the equality of $\langle e^{-i\hat{\varphi}(t)}e^{i\varphi(t)}\rangle = \langle e^{i\hat{\varphi}(t)}e^{-i\hat{\varphi}(t)}\rangle = 1$, we have

$$J^{g^a_2}_L(t) = 0. \tag{B3}$$

But this does not hold for $g^a_3(t,t')$, which is written as

$$\begin{aligned} g^a_3(t,t') &= ig^{<}_{q\alpha 0}(t,t')g^a_{ec}(t,t') \\ &= -if(\varepsilon)\theta(t'-t)e^{-i\varepsilon_{q\alpha 0}(t-t')} \\ &\quad\times[\langle e^{-i\hat{\varphi}(t)}e^{i\hat{\varphi}(t')}\rangle - \langle e^{i\hat{\varphi}(t')}e^{-i\hat{\varphi}(t)}\rangle]. \end{aligned} \tag{B4}$$

Similarly, we derive the current for $g^a_3(t,t')$,

$$J^{g^a_3}_L(t) = \frac{2e\Gamma^L}{\hbar}\mathrm{Im}\int\frac{d\varepsilon}{2\pi}\int dt_1 G^{<}(t,t_1)f(\varepsilon)e^{-i\varepsilon(t_1-t)}\theta(t-t_1) \times[\langle e^{-i\hat{\varphi}(t_1)}e^{i\hat{\varphi}(t)}\rangle - \langle e^{i\hat{\varphi}(t)}e^{-i\hat{\varphi}(t_1)}\rangle]. \tag{B5}$$

Clearly, one can see that the current is nonvanishing. If this term is included in the formula, it is difficult to give analytical expressions of the self-energy, Green's function, and current. So we discuss the condition in which the contribution of this

term to the current is small. To that end, we consider the identity

$$\langle e^{i\hat{\varphi}(t)}e^{-i\hat{\varphi}(t_1)}\rangle = \langle e^{-i\hat{\varphi}(t_1)}e^{i\hat{\varphi}(t+i\hbar\beta)}\rangle, \tag{B6}$$

where $\beta = 1/k_BT$.

From the above relation, one can see that, due to the small value of $\hbar$, the quantity of $\hbar\beta$ is actually negligibly small. Unless the temperature in experiment is zero or negligibly small, one can make a reasonable approximation,

$$\langle e^{i\hat{\varphi}(t)}e^{-i\hat{\varphi}(t_1)}\rangle \approx \langle e^{-i\hat{\varphi}(t_1)}e^{i\hat{\varphi}(t)}\rangle. \tag{B7}$$

In such a case, the current from g_3^a becomes zero, i.e.,

$$J_L^{g_3^a}(t) = 0. \tag{B8}$$

APPENDIX C: THE FORMULA OF THE SPIN CURRENT

In the following, we will derive the spin current arising from the rotating magnetic field by using the Green's function method. The current operator of the α lead in spin space is written as

$$\hat{J}_{\alpha\sigma\sigma'} = -i\sum_k [V_{q\alpha}\hat{c}^\dagger_{q\alpha\sigma}\hat{d}_{\sigma'} - V^*_{q\alpha}\hat{d}^\dagger_\sigma \hat{c}_{q\alpha\sigma'}]. \tag{C1}$$

The spin current is obtained by averaging the current operator from Eq. (C1),

$$\begin{aligned} I_{\alpha\sigma\sigma'}(t) &= \langle \hat{J}_{\alpha\sigma\sigma'}(t)\rangle \\ &= -\sum_q [V_{q\alpha}G^<_{d\sigma,q\alpha\sigma'}(t,t) - V^*_{q\alpha}G^<_{q\alpha\sigma',d\sigma}(t,t)]. \end{aligned} \tag{C2}$$

The lesser Green's functions take the form

$$\begin{aligned} G^<_{d\sigma,q\alpha\sigma'}(t,t) = \int dt_1 V^*_{q\alpha}\big[&G^r_{\sigma\sigma'}(t,t_1)g^<_{q\alpha\sigma'\sigma'}(t_1,t) \\ &+ G^r_{\sigma\sigma'}(t,t_1)g^<_{q\alpha\sigma'\sigma'}(t_1,t)\big], \end{aligned} \tag{C3}$$

$$\begin{aligned} G^<_{q\alpha\sigma',d\sigma}(t,t) = \int dt_1 V^*_{q\alpha}\big[&g^<_{q\alpha\sigma'\sigma'}(t,t_1)G^a_{\sigma'\sigma}(t_1,t) \\ &+ g^r_{q\alpha\sigma'\sigma'}(t,t_1)G^<_{\sigma'\sigma}(t_1,t)\big]. \end{aligned} \tag{C4}$$

Substituting Eqs. (C3) and (C4) into Eq. (C2) and then employing double-time Fourier transformation, we obtain

$$\begin{aligned} I_{\alpha\sigma\sigma'}(t) = -\int \frac{dE_1dE_2dE_4}{(2\pi)^3}e^{i(E_4-E_1)t}\big\{\big[&G^r_{\sigma\sigma'}(E_1,E_2) \\ - G^a_{\sigma\sigma'}(E_1,E_2)\big]\Sigma^<_{\alpha\sigma'\sigma'}(E_2,E_4) + G^<_{\sigma\sigma'}(E_1,E_2) \\ \times\big[\Sigma^a_{\alpha\sigma'\sigma'}(E_2,E_4) - \Sigma^r_{\alpha\sigma'\sigma'}(E_2,E_4)\big]\big\}. \end{aligned} \tag{C5}$$

After averaging over t in Eq. (C5), we obtain the spin current

$$\begin{aligned} &\big\langle I^\nu_{\alpha,\uparrow\uparrow}(t)\big\rangle \\ &= -\big\langle I^\nu_{\alpha,\downarrow\downarrow}(t)\big\rangle \\ &= \sum_n^\infty p^\nu_{\rm tot}[n]\Gamma\Gamma^\alpha \int \frac{dE}{2\pi}\left|\frac{\gamma_s G^{0r}_{\downarrow\downarrow}(E)G^{0r}_{\uparrow\uparrow}(E+\omega)}{1-\gamma_s^2 G^{0r}_{\downarrow\downarrow}(E)G^{0r}_{\uparrow\uparrow}(E+\omega)}\right|^2 \\ &\quad\times[f(E+n\omega) - f(E+\omega+n\omega)], \end{aligned} \tag{C6}$$

with ν representing each type of cavity state. Two Green's functions are used, i.e.,

$$G^{0r}_{\uparrow\uparrow}(E+\omega) = \frac{1}{E+\omega-\varepsilon_0-B_0\cos\theta+i\Gamma/2}, \tag{C7}$$

$$G^{0r}_{\downarrow\downarrow}(E) = \frac{1}{E-\varepsilon_0+B_0\cos\theta+i\Gamma/2}. \tag{C8}$$

[1] A.-P. Jauho, N. S. Wingreen, and Y. Meir, Phys. Rev. B **50**, 5528 (1994).
[2] Q.-F. Sun and T.-H. Lin, Phys. Rev. B **56**, 3591 (1997).
[3] B. Dong, H. L. Cui, and X. L. Lei, Phys. Rev. B **69**, 205315 (2004).
[4] M. M. Odashima and C. H. Lewenkopf, Phys. Rev. B **95**, 104301 (2017).
[5] M. Ridley and R. Tuovinen, Phys. Rev. B **96**, 195429 (2017).
[6] A. Purkayastha and Y. Dubi, Phys. Rev. B **96**, 085425 (2017).
[7] M. Ridley, A. MacKinnon, and L. Kantorovich, Phys. Rev. B **95**, 165440 (2017).
[8] J.-R. Souquet, M. J. Woolley, J. Gabelli, P. Simon, and A. A. Clerk, Nat. Commun. **5**, 5562 (2014).
[9] X. Chen, D. Liu, W. Duan, and H. Guo, Phys. Rev. B **87**, 085427 (2013).
[10] P. K. Tien and J. P. Gordon, Phys. Rev. **129**, 647 (1963).
[11] L. P. Kouwenhoven, S. Jauhar, J. Orenstein, P. L. McEuen, Y. Nagamune, J. Motohisa, and H. Sakaki, Phys. Rev. Lett. **73**, 3443 (1994).
[12] D. Zambrano, L. Rosales, A. Latgúe, M. Pacheco, and P. A. Orellana, Phys. Rev. B **95**, 035412 (2017).
[13] J. R. Tucker and M. J. Feldman, Rev. Mod. Phys. **57**, 1055 (1985).
[14] J. Gabelli and B. Reulet, Phys. Rev. Lett. **100**, 026601 (2008).
[15] R. Hanson, L. M. K. Vandersypen, L. H. Willems van Beveren, J. M. Elzerman, I. T. Vink, and L. P. Kouwenhoven, Phys. Rev. B **70**, 241304(R) (2004).
[16] J. R. Petta, A. C. Johnson, C. M. Marcus, M. P. Hanson, and A. C. Gossard, Phys. Rev. Lett. **93**, 186802 (2004).
[17] K. R. Motes, R. L. Mann, J. P. Olson, N. M. Studer, E. A. Bergeron, A. Gilchrist, J. P. Dowling, D. W. Berry, and P. P. Rohde, Phys. Rev. A **94**, 012344 (2016).
[18] J. P. Olson, K. P. Seshadreesan, K. R. Motes, P. P. Rohde, and J. P. Dowling, Phys. Rev. A **91**, 022317 (2015).
[19] B. Wang, J. Wang, and H. Guo, Phys. Rev. B **67**, 092408 (2003).
[20] P. Zhang, Q.-K. Xue, and X. C. Xie, Phys. Rev. Lett. **91**, 196602 (2003).
[21] H. Yu and J.-Q. Liang, Phys. Rev. B **72**, 075351 (2005).
[22] M. Trif, V. N. Golovach, and D. Loss, Phys. Rev. B **77**, 045434 (2008).
[23] N. Sergueev, Q.-F. Sun, H. Guo, B. G. Wang, and J. Wang, Phys. Rev. B **65**, 165303 (2002).

[24] F. Mireles and G. Kirczenow, Phys. Rev. B **64**, 024426 (2001).
[25] P. Stadler, W. Belzig, and G. Rastelli, Phys. Rev. B **91**, 085432 (2015).
[26] A. Pulkin and O. V. Yazyev, Phys. Rev. B **93**, 041419(R) (2016).
[27] A. Dankert, J. Geurs, M. V. Kamalakar, S. Charpentier, and S. P. Dash, Nano Lett. **15**, 7976 (2015).
[28] B. Zhou, B. Zhou, D. Tang, and G. Zhou, J. Appl. Phys. **115**, 154310 (2014).
[29] Z. Wang, J. Shan, and K. F. Mak, Nat. Nanotechnol. **12**, 144 (2017).
[30] J. B. de Oliveira, I. S. S. de Oliveira, J. E. Padilha, and R. H. Miwa, Phys. Rev. B **97**, 045107 (2018).
[31] K.-R. Jeon, C. Ciccarelli, A. J. Ferguson, H. Kurebayashi, L. F. Cohen, X. Montiel, M. Eschrig, J. W. Robinson, and M. G. Blamire, Nat. Mater. **17**, 499 (2018).
[32] S. J. Magorrian, V. Zólyomi, and V. I. Fal'ko, Phys. Rev. B **96**, 195428 (2017).
[33] R. Cheng, J. Xiao, Q. Niu, and A. Brataas, Phys. Rev. Lett. **113**, 057601 (2014).
[34] J.-C. Rojas-Sánchez, S. Oyarzún, Y. Fu, A. Marty, C. Vergnaud, S. Gambarelli, L. Vila, M. Jamet, Y. Ohtsubo, A. Taleb-Ibrahimi, P. Le Fèvre, F. Bertran, N. Reyren, J.-M. George, and A. Fert, Phys. Rev. Lett. **116**, 096602 (2016).
[35] L. Thomas, M. Benzaouia, S. Serrano-Guisan, G. Jan, S. Le, Y. Lee, H. Liu, J. Zhu, J. Iwata-Harms, R. Tong *et al.*, in *2017 IEEE International Magnetics Conference (INTERMAG)* (IEEE, Piscataway, NJ, 2017), p. 1.
[36] E. Moen and O. T. Valls, Phys. Rev. B **97**, 174506 (2018).
[37] S. Peng, W. Kang, M. Wang, K. Cao, X. Zhao, L. Wang, Y. Zhang, Y. Zhang, Y. Zhou, K. L. Wang *et al.*, IEEE Magn. Lett **8**, 3105805 (2017).
[38] A. Mellnik, J. Lee, A. Richardella, J. Grab, P. Mintun, M. H. Fischer, A. Vaezi, A. Manchon, E.-A. Kim, N. Samarth *et al.*, Nature (London) **511**, 449 (2014).
[39] Y. Xiao and H. Guo, Phys. Can. **72**, 81 (2016).
[40] B. M. Yao, Y. S. Gui, Y. Xiao, H. Guo, X. S. Chen, W. Lu, C. L. Chien, and C. M. Hu, Phys. Rev. B **92**, 184407 (2015).
[41] A. D. Armour, M. P. Blencowe, E. Brahimi, and A. J. Rimberg, Phys. Rev. Lett. **111**, 247001 (2013).
[42] S. Dambach, B. Kubala, V. Gramich, and J. Ankerhold, Phys. Rev. B **92**, 054508 (2015).
[43] B. Kubala, V. Gramich, and J. Ankerhold, Phys. Scr. **2015**, 014029 (2015).
[44] O. Parlavecchio, C. Altimiras, J.-R. Souquet, P. Simon, I. Safi, P. Joyez, D. Vion, P. Roche, D. Esteve, and F. Portier, Phys. Rev. Lett. **114**, 126801 (2015).
[45] L. Henriet, A. N. Jordan, and K. Le Hur, Phys. Rev. B **92**, 125306 (2015).
[46] M. Mecklenburg, B. Kubala, and J. Ankerhold, Phys. Rev. B **96**, 155405 (2017).
[47] H. K. Zhao and J. Wang, Eur. Phys. J. B **9**, 513 (1999).